# Full test of the DVCS electronics for E12-06-114 Run 2014-2015

A. Camsonne, C.E. Hyde, P. King, C. Muñoz Camacho, J. Roche

(Dated: Sep 8, 2014)

We summarize herein the tests of the DVCS trigger module and ARS sampling electronics in a configuration very similar to the final experimental setup. This document is in response to the recommendation to perform a Full System Test by July 25, from the report on the DVCS Trigger Review that took place on May 20 (2014).

## CONTENTS

## I. DVCS SETUP IN TEST LAB

The DVCS calorimeter and its ancillary electronics were installed and tested in the Test Lab until the move to the Hall on Aug 1st. Signals from the $PbF_2$ blocks were obtained from either cosmics rays passing through the calorimeter or from pulsed LEDs placed in front of them. Fig. 1 are pictures of the hardware assembly, and Fig. 2 shows a view of the LED panel used to generate signals to feed the trigger module.

FIG. 1. Left: overview of the DVCS setup in the Test Lab. Right: Front view of the calorimeter, showing the array of 208 $PbF_2$ blocks.

Fig. 3 is a diagram of the trigger module internal logic. An accepted trigger is formed on the leading edge of the "Master OR" signal if:

- "TSLive" is true;
- "ExtBusy" is false;
- "TrigFifoFull" is false;
- and "Busy" is false.

On an accepted trigger:

- "Busy" is set to be true;
- "ARS stop" is turned on;
- the ADC gate is sent to the calorimeter cluster-finding circuit;
- after 500 ns, the calorimeter trigger is tested for a valid cluster;

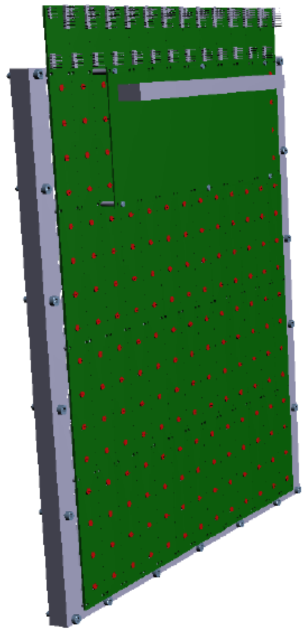

FIG. 2. A panel with 208 LEDs (one in front of each calorimeter block) was used to test the trigger module and its clustering algorithm.

- If there is a valid cluster:
  - "ARS valid" is turned on, and it will remain on for 138 $\mu$s;
  - "ARS stop" will also remain on 138 $\mu$s;
- If there is not a valid cluster:
  - "ARS stop" will stop 800 ns after it was started;
- "Busy" stays on until 140 ns after the end of "ARS Stop".

The DAQ control signals for the TestLab DAQ are such that the DVCS trigger crate is responsible for all trigger processing, and the ROCs are secondary.

Fig. 4 shows the control signals running between the DVCS trigger crate, NIM crate, and ROCs. The first channel of the gate generator now plays the role of the "TS live" signal; it is in flip-flop mode, to set "TS live" enable the gate, and disable the gate to remove the live signal. The ROC busy signals are now input to the DVCS trigger crate. The ROC triggers are generated from the ARS valid signal. The TDC trigger is also derived from the ARS valid signal.

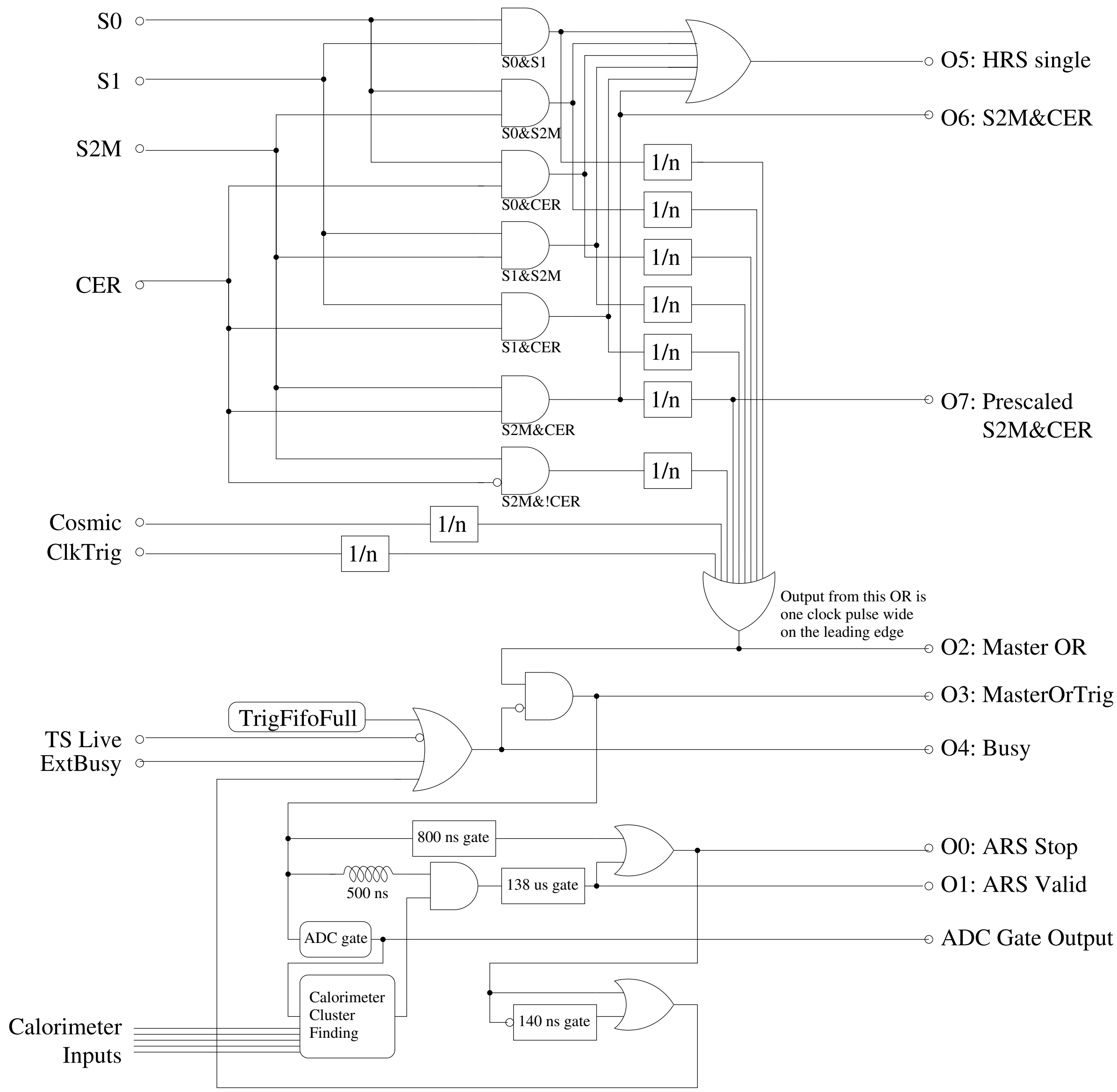


FIG. 3. Diagram of the trigger module internal logic.

## II. FULL READOUT IMPLEMENTATION (TRIGGER MODULE + ARS)

A simultaneous readout of the trigger module and all ARS modules was successfully implemented in the Test Lab. The trigger module was read from one VME crate and the 16 ARS modules were readout from a different crate. Fig. 5 shows the correlation between the ARS and trigger module for an LED run. The correlation shows the successful implementation of the combined readout of all the modules and the synchronization of the events between the different crates. The associated decoding software for data analysis was also tested and debugged during these tests.

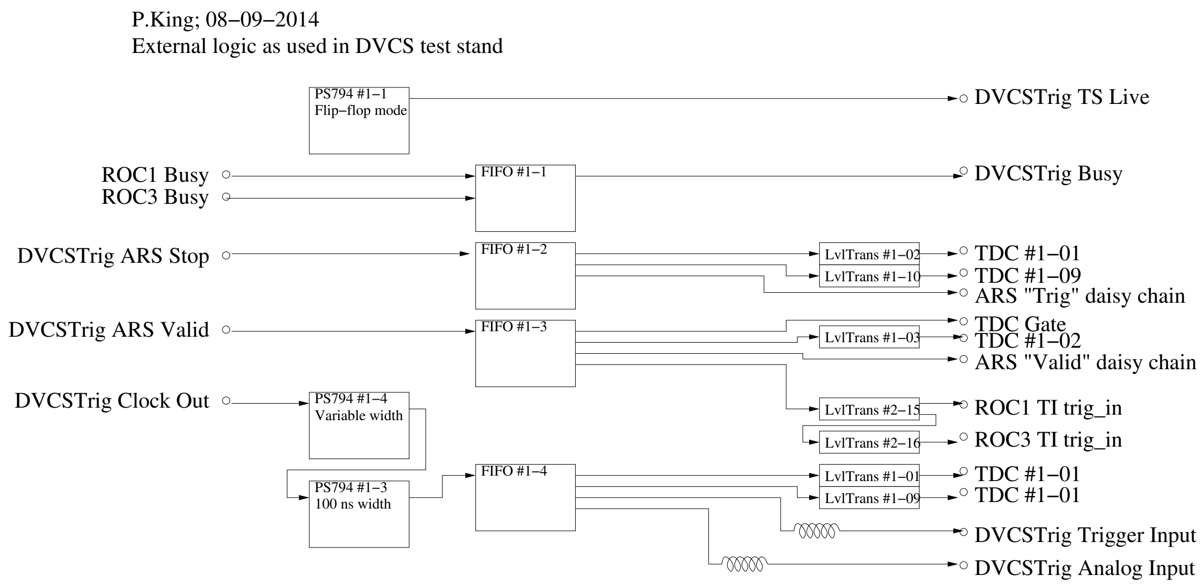


FIG. 4. External logic as used in DVCS test stand.

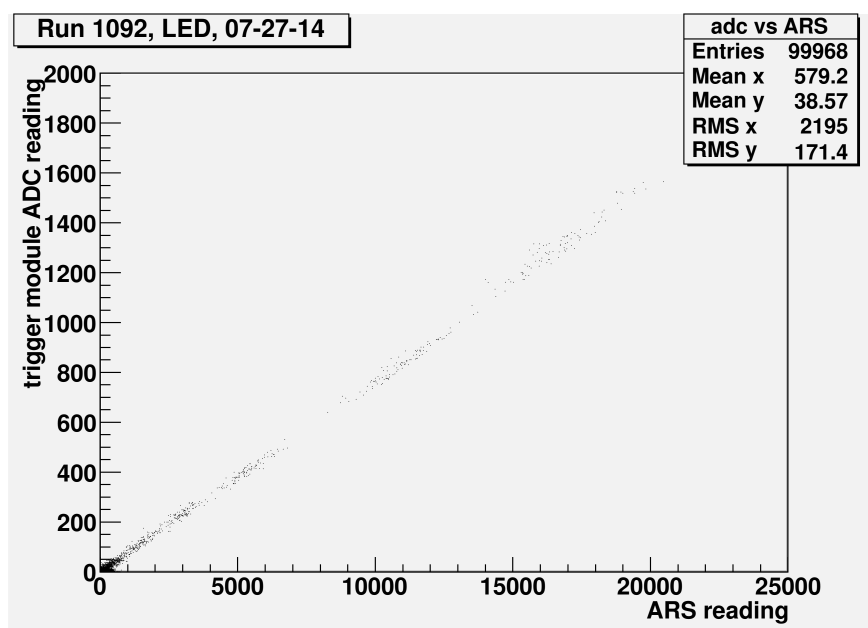


FIG. 5. Trigger module *vs*. the ARS readouts. The correlation between the two sets of electronics shows the correct implementation of a combined DAQ and the synchronization of the events.

## III. CLUSTERING ALGORITHM

The proper computation of clusters has been thoroughly tested using LED runs and changing the clustering threshold. For these tests, the clock input was used as trigger source.

This input is always validated regardless of whether a cluster is found or not. However, the clusters are computed in the usual way and the existence or not of a cluster above the threshold is reported in the data stream. The use of the clock input simply allows us to check whether some clusters that should have been reported were not. This provides a way to evaluate the potential inefficiency of the module.

During the LED runs, an LED is flashed sequentially in front of each of the calorimeter blocks. Clusters of 2×2 blocks are computed by the trigger module and the existence of a cluster is reported if at least one of them is above a programmable threshold. Fig. 6 (top) shows the signal recorded by each of the channels of the calorimeter during the run. The LED flashed at each event will primarily create a signal in one PMT at a time, but neighboring blocks will also detect some leakage light of lower intensity. By performing several LED scans at different trigger thresholds, the clustering algorithm was successfully tested. Fig. 6 (bottom) shows the results of three runs at threshold values of 200, 400 and 600 (ADC channels). The number of times that each of the clusters of the calorimeter had a maximum signal (typically the LED was flashing in front of the 2×2 corresponding blocks) is shown in the 2D-histograms (Fig. 6, bottom), for different values of the threshold. From the total number of events in the 3 runs (∼310k) no single cluster was reported incorrectly neither way. Around 134k events found a cluster correctly and ∼176k events contained no cluster and the module reported this correctly. All areas of the calorimeter are roughly covered by this test at either one of the thresholds. The results of these tests show the good performance of the clustering algorithm, including clusters that overlap between two different FPGAs, which shows the data flows correctly and reliably inside the trigger module.

## IV. CALORIMETER CALIBRATION: COSMIC RUNS

By using minimum-ionizing cosmic rays, we performed a relative calibration of the gains of each channel. The energy loss by cosmics passing vertically through the 3-cm-long $PbF_2$ blocks is around 30 MeV. Fig. 7 shows a typical event, as seen by the trigger module. Fig. 8 (top) shows the energy distribution in each of the 16 blocks of one of the calorimeter columns, as recorded by the ARS modules. Vertical cosmics were selected by requiring a signal in both the top and bottom block of the same column. By modifying the high voltage of each PMT, we were able to adjust the mean of each distribution to a common value to better than 3%, as shown in Fig. 8 (bottom).

## V. TRIGGER SIGNAL TIMING FOR VALID AND INVALID TRIGGERS

For this test, an analog signal is sent simultaneously to the S2m input of the trigger module, one of the ADC channels of the trigger module and one of the channels of one of the ARS modules. The trigger was configured to require clusters, with a cluster threshold of 500. By increasing or decreasing the attenuation of the trigger module ADC input, we could generate either valid or invalid triggers.

We used a relative delay on the S2m trigger input of 32 ns, as that had been found

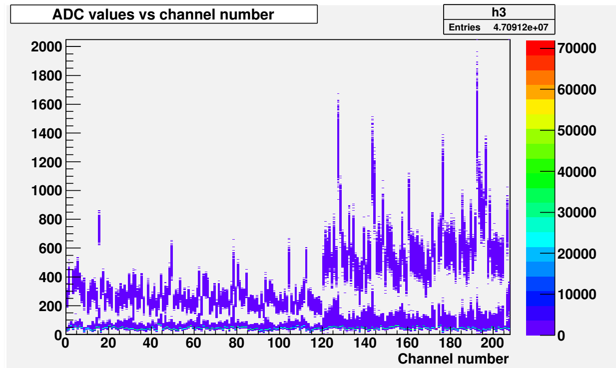


(a) ADC value recorded by the trigger module for a typical LED run, as a function of the calorimeter channel number.

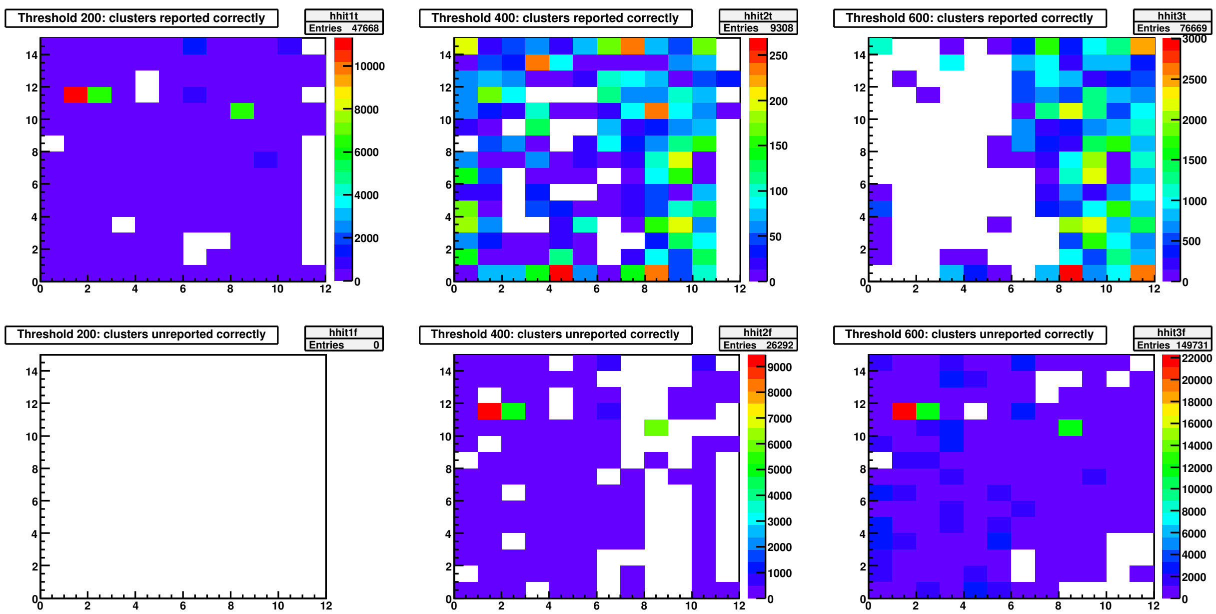


(b) For three different values of the threshold (columns), position of the highest signal cluster when the existence of a cluster was correctly reported (top) and when the absence of a cluster above threshold was correctly reported (bottom). Both cases are successfully tested across the surface of the calorimeter at some value of the threshold. Not a single event was reported incorrectly.

FIG. 6. Clustering algorithm tests.

previously to give an optimized ADC reading in the trigger crate.

## A. Signal timing for valid triggers

Starting with an integration gate setting of 7, yielding a gate width of about 35 ns, there is about 560 ns delay between the ARS stop and the ARS valid for a valid trigger. This is the time that the trigger module takes to determine the validity of a trigger. In Fig. 9 the

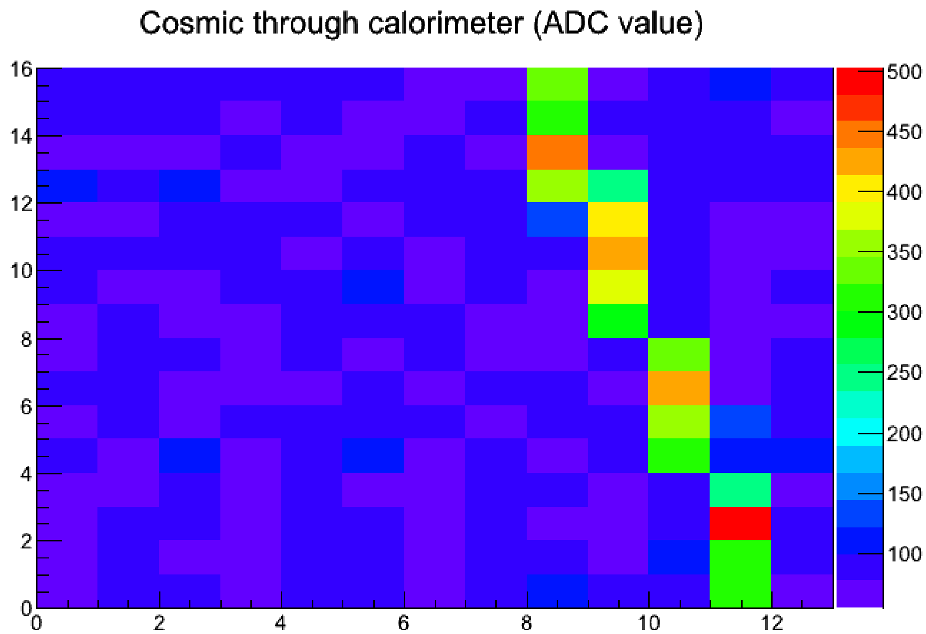


FIG. 7. Cosmic ray travelling through the calorimeter, as seen by the trigger module. The energy scale shows the ADC value recorded by the module.

trigger is a copy of the original trigger source, and the time between it and the ARS stop does not take into account the cable delay on the way to the trigger input. When the event is valid, both the ARS stop and ARS valid are true for about 140 $\mu$s, and they stop within a few ns of each other (Fig. 9, bottom).

### B. Comparison of signal timing for invalid triggers

When the attenuator is adjusted to make invalid triggers, the ARS stop ends about 850 ns after it starts. This is about 280 ns after the time when the ARS valid would be asserted if the event was valid (see Fig. 10).

### C. Increased gate width to 350 ns

When we change the integration gate width setting to 70 (350 ns), we see the ARS valid transition is pushed later, but so is the end of the ARS stop for invalid triggers. The relative timing of the "invalid" ARS stop and the beginning of the ARS valid remains about 290 ns, independent of the gate width (see Fig. 11). However, we will need to adjust the ARS parameters to expect a valid delay appropriate to the chosen gate setting.

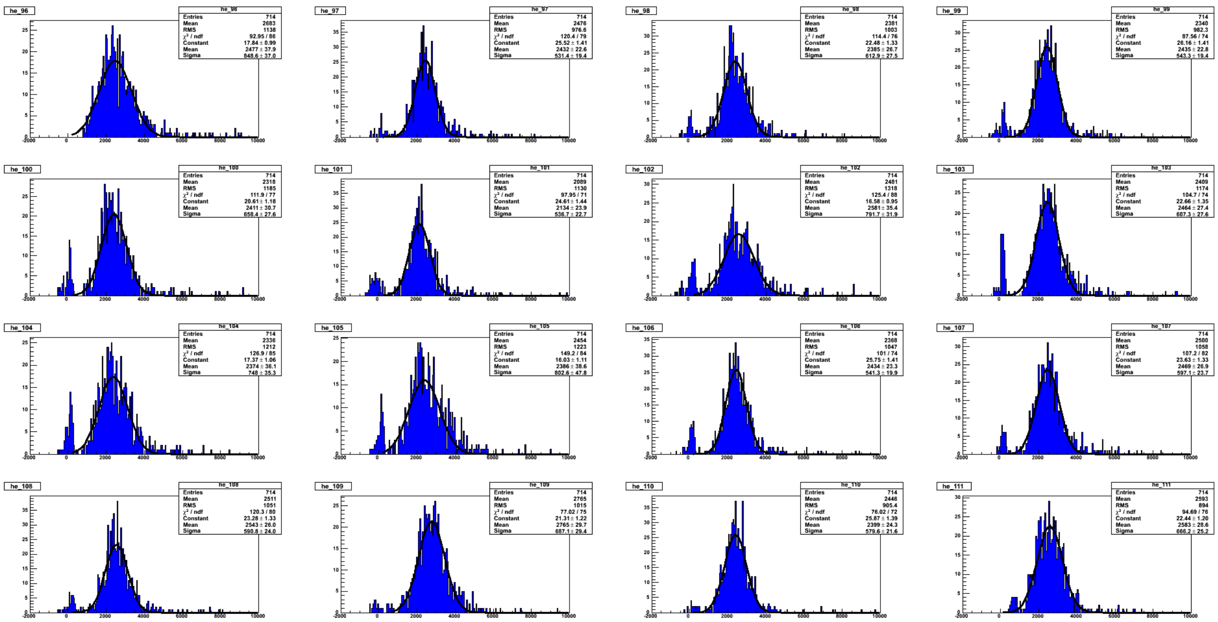

(a) Energy loss by cosmics in each of the 16 blocks of one calorimeter column. A cut on the energy loss in the top and bottom block is applied in order to select vertical events.

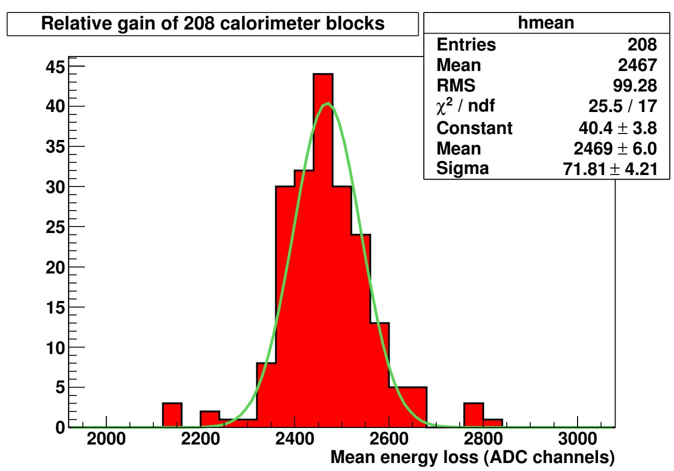


(b) Histogram of the average energy loss in each of the 208 calorimeter blocks after adjusting the gains of each channel. The spread is around 3%.

FIG. 8. Calorimeter calibration with cosmic rays. The relative gain of all channels is adjusted to better than 3%.

## VI. TRIGGER INPUT COMBINATIONS

We have checked that we see events taken for all sensible combinations of input trigger[1]. We note that all of the "Clock" counters increment for all triggers. Tab. I shows which

[1] In these data, the trigger crate did not have any input cards installed, so we used a global trigger of zero, disabled clustering, and we had all prescales set to 1.

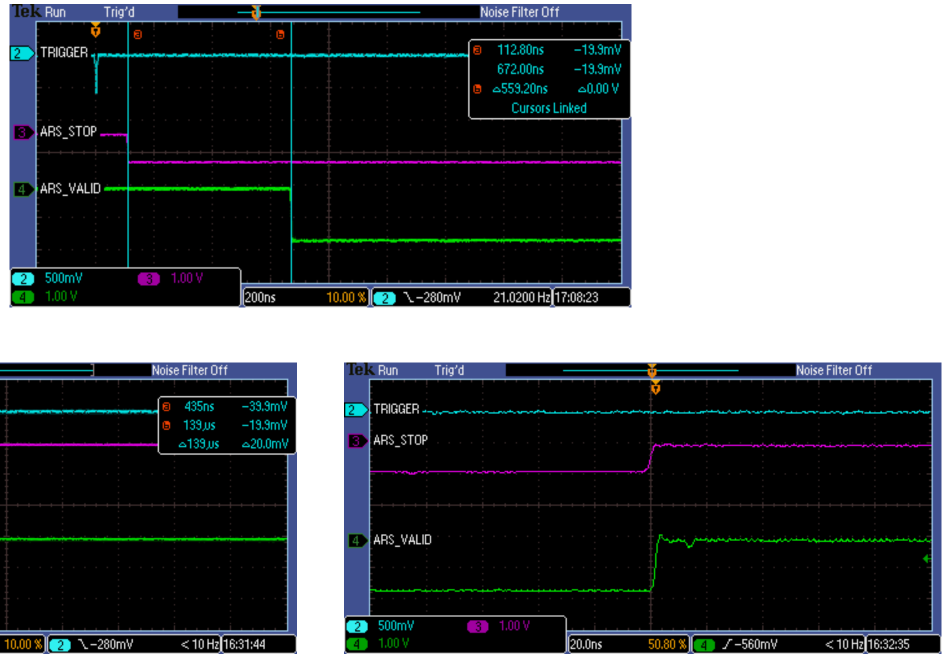


FIG. 9. Signal timing for valid triggers. There is about 560 ns between the ARS stop and the ARS valid for a valid trigger. The ARS stop and valid are true for about 140 $\mu$s.

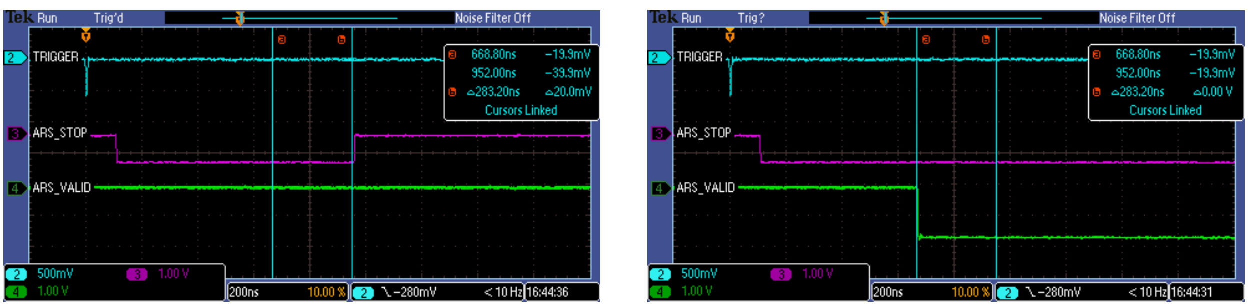


FIG. 10. For invalid triggers the ARS stop ends about 850 ns after it starts, which is about 280 ns after the time when the ARS valid would have been asserted.

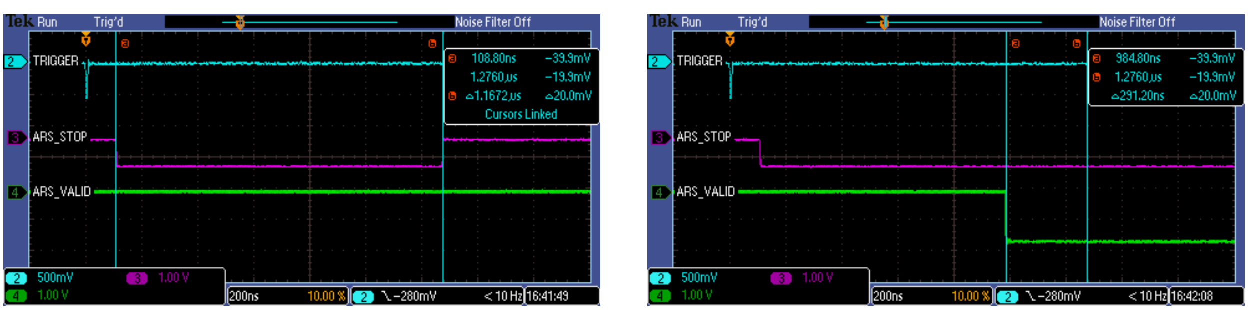


FIG. 11. Timing for an increased gate of 350 ns. The ARS valid and the end of the ARS stop for invalid trigger are pushed later. Their relative timing remains constant ($\sim$290 ns) regardless of the gate width.

| Event | TrigPattern | InputCombination | Notes |
|---|---|---|---|
| = | =========== | ================ | ===== |
| Y | "01" | cosmic | |
| Y | "02" | clock | |
| N | ---- | S0 | counter increments on singles |
| N | ---- | S1 | counter increments on singles |
| Y | "10" | S2m | |
| N | ---- | Cer | counter increments on singles |
| = | =========== | ================ | ===== |
| Y | "0c" | s0 & s1 | |
| Y | "14" | s0 & s2m | |
| Y | "24" | s0 & cer | |
| Y | "18" | s1 & s2m | |
| Y | "28" | s1 & cer | |
| Y | "30" | s2m & cer | |
| = | =========== | ================ | ===== |
| Y | "1c" | s0 & s1 & s2m | |
| Y | "34" | s0 & s1 & cer | |
| Y | "38" | s1 & s2m & cer | |
| = | =========== | ================ | ===== |
| Y | "03" | cosmic & clock | |

TABLE I. Tests of different trigger input combinations. Everything responds as expected.

combinations generate a triggered event and what trigger pattern is recorded in that event. Everything works the way we would expect.

## VII. DATA RATE

Data transfer tests were performed in the Test Lab with 13 ARS modules in one single crate. The average data rate was ~850 Hz. The setup that we have just assembled in the Hall will have 3 different crates to share the 13 ARS modules and is expected to be able to saturate at around 2 kHz.

The next step is to repeat these tests in the Hall, as well as to quantify the effect of deadtime.

## VIII. REPLY TO COMMITTEE'S SUGGESTIONS

### A. Analog sum trigger alternative

The committee suggested that the possibility of building a simple analog photon trigger should be studied as an alternative to using the DVCS trigger module. To do so, we used 2010 DIS data (triggered with the HRS only with no selection on the calorimeter readout). The ARSs record the voltage versus time trace produced by each block of the DVCS calorimeter over 128 ns with a 1 ns resolution. On the one hand, one can compute the integral of the trace for each block, mimicking the ADC reading of the DVCS trigger module. From these integrated traces, one can compute the 198 $2\times2$ tower sums on which the DVCS trigger module applies its threshold test. On the other hand, one can sum bin-per-bin the 208 ARS traces mimicking the overall analog sum signal that would be sent to the discriminator. Fig. 12 shows the correlation between the tower with largest integrated signal and the amplitude of the summed analog signal. In this situation, a 1 GeV threshold on the integrated ADC signal (mimicking the DVCS trigger module) would remove most of the noise while to achieve the same selection a 3 GeV threshold should be applied on the analog sum signal. For this kinematics, the average energy of the DVCS photon is 3 GeV, making the analog sum photon trigger a less than ideal alternate triggering scheme.

### B. Fans and cooling

A fan has been installed under the trigger module, and the temperature of the system has decreased significantly.

## IX. CONCLUSION AND OUTLOOK

The DVCS collaboration feels that the trigger module firmware is fully debugged and the unit is working properly. A full implementation of the DVCS electronics, including both the trigger module and the ARS sampling system has been successfully tested in the Test Lab. Timings and data rates are as expected.

We are currently installing everything in the Hall, where we would be able to measure the deadtime of the acquisition chain in the experimental running conditions. We will report on the results by the deadline of Sep 26 set by the committee.

## X. ACKNOWLEDGEMENTS

The DVCS collaboration would like to wholeheartedly thank Benjamin Raydo for his extensive work on the trigger module firmware and hardware, leading to the stable and

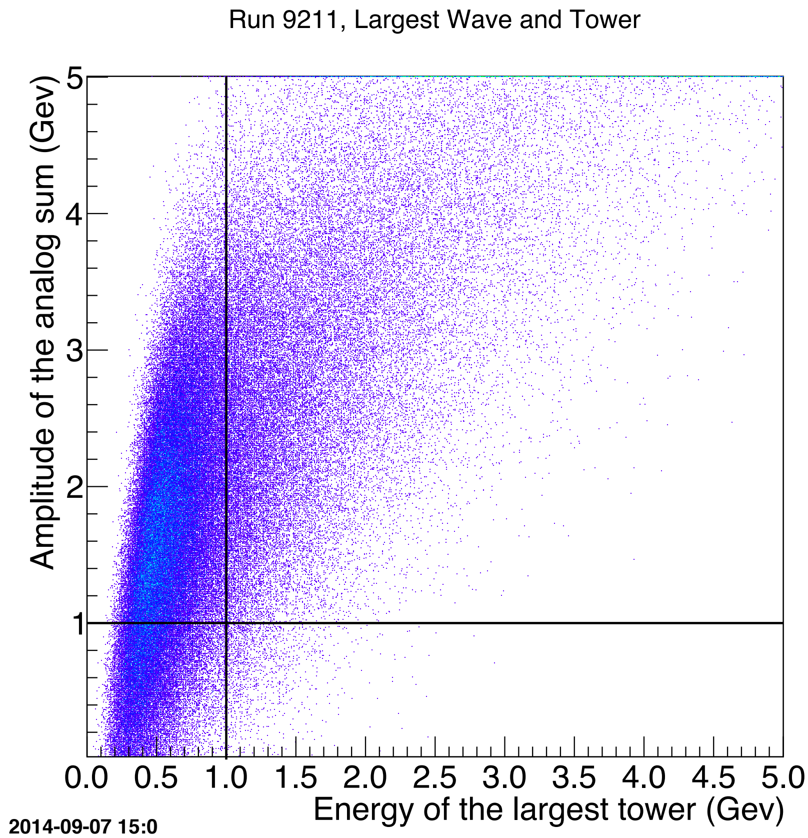


FIG. 12. Analog sum *vs.* largest 2×2 cluster, from DIS data taken during the 2010 DVCS run. The analog sum contains too much noise to make it an efficient trigger for the experiment.

functional version this document reports on.